Available online at www.sciencedirect.com

SCIENCE DIRECT®

ELSEVIER

Chemical Physics Letters 367 (2003) 207–213

CHEMICAL PHYSICS LETTERS

www.elsevier.com/locate/cplett

Classification of reaction pathways via momentum–space and quantum molecular similarity measures

Lluís Amat [a], Ramon Carbó-Dorca [a], David L. Cooper [b], Neil L. Allan [c,*]

[a] Institute of Computational Chemistry, University of Girona, 17071 Girona, Spain
[b] Department of Chemistry, University of Liverpool, Liverpool L69 7ZD, UK
[c] School of Chemistry, University of Bristol, Cantock's Close, Bristol BS8 1TS, UK

Received 1 October 2002

Abstract

For four rearrangement reactions, we evaluate (i) values of the moments of momentum $\langle p^n \rangle (-2 \leqslant n \leqslant +1)$ for reactants, products and transition states (ii) position–space similarity indices between reactants, products and transition states using wavefunctions generated from both Hartree–Fock and density-functional theory (B3LYP). Both the momentum–space expectation values and the similarity measures can be used to distinguish Hammond and anti-Hammond behaviour. In position–space, two new parameters, δ and ϕ, are introduced to quantify the position and character of the transition state relative to the reactants and products.

1. Introduction

There is a still a need for interpretative tools to analyse, to compare and to obtain chemical insight from the molecular wavefunctions and densities calculated by increasingly accurate techniques. Position, r-space electron density plots, for example, have been used for many years to visualize electronic structure. Although much less attention has been paid to the momentum, p-space representation, the chemically interesting information available in momentum–space density plots of small molecules (at equilibrium geometry [1–3] and over a wide range of nuclear separation [4]) and of large molecules such as polyenes [5] have been discussed previously. In addition, quantum similarity techniques in which r- or p-space electron densities are compared quantitatively via a variety of similarity and dissimilarity indices have been useful in applications [6–12], mostly, but not exclusively, in the rationalization and prediction of drug activity.

In this Letter, we extend these studies to reactivity and consider changes of momentum–space quantities and similarity indices along reaction pathways. The variation of both p-space expectation values and of ab initio r-space quantum molecular similarity measures are examined along the reaction pathway of four simple gas-phase intramolecular rearrangement reactions, F_2S_2/FSSF,

---

[*] Corresponding author. Fax: +44-117-925-1295.
E-mail address: n.l.allan@bristol.ac.uk (N.L. Allan).

0009-2614/02/$ - see front matter © 2002 Elsevier Science B.V. All rights reserved.
PII: S0009-2614(02)01701-3

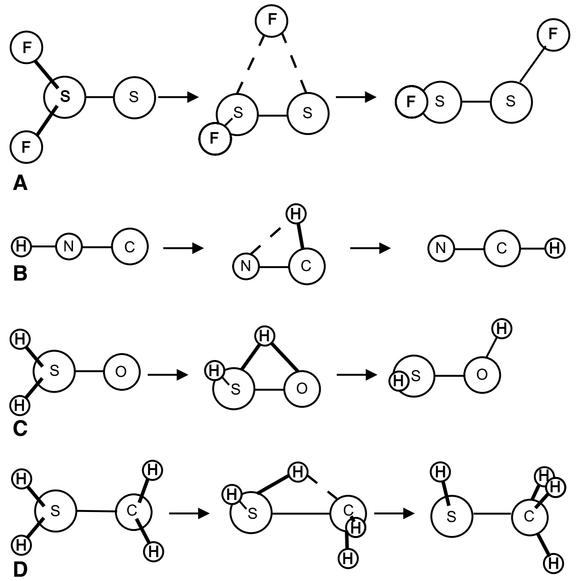

Fig. 1. The four rearrangement reactions.

HNC/HCN, H_2SO/HSOH and H_2SCH_2/$HSCH_3$, which we label reactions (A)–(D) as shown in Fig. 1.

Particular attention is paid to the nature of the transition state of these exothermic reactions. The Hammond postulate [13], widely used in organic chemistry, essentially states that if the transition state (TS) is near in energy to an adjacent stable complex, then it is also similar in structure to that complex. An exothermic reaction would therefore be expected to possess a reactant-like TS while endothermic processes should be characterized by a product-like TS. Rearrangement reactions, normally involving limited nuclear motions, are generally expected to follow the Hammond postulate. Of the four reactions discussed in this Letter, the F_2S_2/FSSF and the HNC/HCN reactions have early transition states and show Hammond-like behaviour. In contrast the H_2SO/HSOH reaction has a late transition state and demonstrates anti-Hammond characteristics [14]. The transition state is structurally more similar to HSOH than to H_2SO, although in energy it is closer to H_2SO. The H_2SCH_2/$HSCH_3$ transition state shows characteristics intermediate between these two types of behaviour. In this Letter, we show how *p*-space quantities and *r*-space similarities can be used to distinguish Hammond and anti-Hammond transition states. In addition, two new parameters, δ and ϕ, readily determined from the quantum molecular similarities, are introduced to quantify the degree of similarity of the transition state both to reactants and to products.

2. Methods

Wavefunctions were generated for the reactants, products and transition states of all the reactions shown in Fig. 1 using self-consistent Hartree–Fock (HF) theory and also density functional theory (DFT) with the B3LYP exchange-correlation functional as implemented in GAUSSIAN 98 [15]. The 6-31G** basis set was used for all atoms.

Relative energies of HF and DFT transition states (TS) and products (P) relative to reactants (R) are collected together in Table 1. In addition the values of the exothermicity factor, γ, defined by Cioslowki [16] as

$$\gamma = (E_P - E_R)/(2E_{TS} - E_R - E_P) \tag{1}$$

Table 1
Calculated relative energies (kcal/mol) and values of γ ($= (E_P - E_R)/(2E_{TS} - E_R - E_P)$) for the four rearrangement reactions studied

	F_2S_2/FSSF	HNC/HCN	H_2SO/HSOH	H_2SCH_2/$HSCH_3$
(a) HF				
$E_{TS} - E_R$	64.5	40.0	50.3	17.9
$E_P - E_R$	−9.6	−9.5	−32.9	−80.2
γ	−0.069	−0.106	−0.246	−0.691
(b) DFT				
$E_{TS} - E_R$	42.8	33.9	38.2	25.9
$E_P - E_R$	−3.6	−13.4	−26.2	−70.0
γ	−0.04	−0.165	−0.255	−0.575

are also listed. This factor, which takes values between +1 and −1, is the ratio of the difference and the sum of the activation energies for the forward and reverse reactions. The H_2SCH_2/$HSCH_3$ rearrangement is both the most exothermic of the four and possesses the most negative γ at both the HF and DFT levels. γ increases in magnitude along the series of reactions (A)–(D) (Fig. 1) and, as might be expected, it does not give any indication of Hammond or anti-Hammond behaviour.

2.1. Momentum space

For molecular systems the most straightforward route to momentum–space quantities is to obtain first the position–space wavefunction $\Psi(\mathbf{r})$ and then to transform it analytically to momentum space as described, for example, in [17]. The Fourier transform that relates $\Psi(\mathbf{r})$ to $\Psi(\mathbf{p})$,

$$\Psi(\mathbf{p}) = \frac{1}{(2\pi)^{3/2}} \int \Psi(\mathbf{r}) \exp(-i\mathbf{p}\cdot\mathbf{r})\, d\mathbf{r}, \tag{2}$$

preserves the form of the wavefunction so that the electron density, individual orbitals, basis functions and the total wavefunction are related to each other in p-space exactly as they are in r-space. In momentum space all explicit information concerning the coordinates of nucleus α is contained in 'phase factor' terms of the form $\exp(-i\mathbf{p}\cdot\mathbf{R}_\alpha)$.

The total molecular electron density $\rho(\mathbf{p})$ decreases rapidly with increasing p, falling off according to a high power of p and so it is dominated by low values of p. This low-p region corresponds in position space to the long-range slowly varying valence electron density. In this Letter, we concentrate on the momentum–space expectation values, the moments of momentum,

$$\langle p^n \rangle = \int p^n \rho(\mathbf{p})\, d\mathbf{p}, \tag{3}$$

which may be evaluated by direct numerical integration. $\langle p^0 \rangle$ $(n = 0)$ is simply the number of electrons. $\langle p^2 \rangle (n = 2)$ is twice the kinetic energy and so, by the virial theorem, in any exothermic reaction $\langle p^2 \rangle$ increases from reactants to products by an amount equal to twice the decrease in the total energy. Decreasing values of n place increasing emphasis on the slower moving valence electrons, and so in this Letter we have chosen to consider moments with $n < 2$.

Our construction of $\rho(\mathbf{p})$ via the Fourier transform of Kohn–Sham orbitals from B3LYP calculations requires a comment. Formally, Kohn–Sham orbitals relate to a 'model' non-interacting system, constrained by a potential that is dependent on the choice of exchange-correlation function. Thus, strictly, in our DFT calculations we examine the electron density of the model system. Even if the model possessed the exact $\rho(\mathbf{r})$, Fourier transformation of the Kohn–Sham orbitals would not lead to the exact $\rho(\mathbf{p})$ [18]. Nevertheless, the 'model system' momentum–space electron densities constructed from the transformed Kohn–Sham orbitals do not differ greatly from the Hartree–Fock $\rho(\mathbf{p})$, and so we have chosen to use these. Furthermore, spherically averaged p-space Kohn–Sham orbitals often give better agreement with (e, 2e) experiments than do their Hartree–Fock counterparts [19].

2.2. Ab initio position–space molecular similarity

We use here the widely used quantum molecular similarity measures (QMSM) between molecules A and B introduced by Carbó and co-workers [20,21], based on integrals of the form

$$Z_{A,B}(\Theta) = \int\int \rho_A(\mathbf{r}_1)\Theta(\mathbf{r}_1, \mathbf{r}_2)\rho_B(\mathbf{r}_2)\, d\mathbf{r}_1\, d\mathbf{r}_2, \tag{4}$$

in which $\Theta(\mathbf{r_1}, \mathbf{r_2})$ is a positive definite operator, set equal here to $1/r_{12}$, i.e., a 'Coulomb-like' QMSM is evaluated. Since the value of $Z_{A,B}$ given by Eq. (4) depends on the relative spatial orientation of molecules A and B, their mutual orientation must be optimized [22] in order to maximize their QMSM.

3. Results

3.1. Momentum space

We consider first the momentum–space quantities for each reaction. A range of HF and DFT moments of momentum $\langle p^n \rangle$ from $n = -2$ to +1

Table 2
Calculated changes in momentum expectation value $\Delta\langle p^n\rangle$ for the transition states (TS) and products (P) of the four rearrangement reactions, relative to the reactants

	$\Delta\langle p^{-2}\rangle$	$\Delta\langle p^{-1}\rangle$	$\Delta\langle p^{3/4}\rangle$	$\Delta\langle p\rangle$
(a) HF				
F_2S_2/FSSF				
TS	0.0574	0.0318	−0.0502	−0.0648
P	−0.0981	−0.0169	0.0004	0.0066
HNC/HCN				
TS	0.3810	0.0873	−0.0474	−0.0675
P	−0.6687	−0.0818	0.0067	0.0062
H_2SO/HSOH				
TS	0.2456	0.0913	−0.0698	−0.0914
P	0.2613	0.0655	−0.0163	−0.0201
H_2SCH_2/$HSCH_3$				
TS	0.9768	0.2859	−0.1422	−0.1759
P	0.2137	0.0387	−0.0096	−0.0056
(b) DFT				
F_2S_2/FSSF				
TS	0.1546	0.0694	−0.0524	−0.0647
P	−0.0746	−0.0314	0.003	0.0047
HNC/HCN				
TS	0.3758	0.0789	−0.0442	−0.0598
P	−0.8270	−0.1002	0.0107	0.0095
H_2SO/HSOH				
TS	0.1152	0.0583	−0.0443	−0.0497
P	0.1854	0.0540	−0.0118	−0.0049
H_2SCH_2/$HSCH_3$				
TS	0.7419	0.2191	−0.1026	−0.1324
P	0.0471	0.0174	0.0025	0.0046

inclusive were evaluated. Table 2 lists key results for changes in p-space expectation values, $\Delta\langle p^n\rangle$, which are defined relative to the *reactants*, for $n = -2, -1, 3/4$ and 1.

All four reactions are exothermic and so the transition state is closer in energy to the reactants than to the products in each case. For HF and DFT densities, the moments of momentum listed in Table 2 and, in particular, the variation of $\langle p^n\rangle$ along the reaction coordinate demonstrate clearly the nature of the transition states and their proximity to reactants or products. Consider, for example, $\Delta\langle p^{-1}\rangle$. For the HNC/HCN and F_2S_2/FSSF rearrangements, the value of $\langle p^{-1}\rangle$ for the transition state is closer to the reactants than to the products, both for the HF and DFT descriptions. For the overall reaction, $\Delta\langle p^{-1}\rangle$ is negative. On the other hand, for the anti-Hammond H_2SO/HSOH reaction, $\langle p^{-1}\rangle$ for the transition state is closer to products than to reactants. The H_2SCH_2/$HSCH_3$ case is intermediate. We note that $\Delta\langle p^{-1}\rangle$ for the overall reaction is positive in these last two examples.

The behaviour of $\Delta\langle p^{-2}\rangle$ is similar, with transition states closer to the reactants for F_2S_2/FSSF and HNC/HCN, but the reverse for the remaining two reactions. Over the anti-Hammond pathway (H_2SO/HSOH) $\langle p^{-2}\rangle$ even *increases* further from the transition state to the products at both the HF and the DFT levels. Thus for the two reactions with early transition states, the values of $\langle p^n\rangle (n = -1, -2)$, which especially emphasize the valence electron density, *increase* from reactants to transition state, although the overall change in these quantities from reactants to products is *negative*.

For positive n, only the $H_2SO/HSOH$ reaction shows a decrease in $\langle p^{3/4}\rangle$ and $< p >$ from reactants to products, and the transition state expectation values are closer to those for the products than to those for the reactants. Again, the $H_2SCH_2/HSCH_3$ case is intermediate between this and the Hammond rearrangements. Fig. 2 shows schematically the observed variations in $\langle p^n\rangle$ with n and the degree of Hammond-like behaviour in the transition state.

The trends in all of the moments of momentum listed in Table 2 demonstrate clearly whether the transition state is closer to the reactants or products, which is not apparent from the total energies listed in Table 1. From each column of values, the position of the transition states is predicted to follow the relative order

$$\underset{\text{Early TS}}{\text{HNC/HCN}} \approx \text{F}_2\text{S}_2\text{/FSSF} < \text{H}_2\text{SCH}_2\text{/HSCH}_3 < \underset{\text{Late TS}}{\text{H}_2\text{SO/HSOH}}$$

3.2. Position space

How do r-space similarity indices reflect these trends? Once $Z_{A,B}$ (Eq. (4)) has been evaluated there are a number of possible ways of proceeding. The first is the calculation of the Carbó similarity index [20], $I_{A,B}$, according to

$$I_{A,B} = Z_{A,B}/(Z_{A,A}Z_{B,B})^{1/2}. \quad (5)$$

In examples such as those considered here, A and B may be reactant and product, reactant and transition state, or product and transition state, respectively, and the values of $I_{A,B}$ for each reaction are all close to unity, as shown in the first three columns of Table 3. It is helpful instead to introduce a ‘distance’-like measure of the difference between the electron densities of A and B

$$d_{A,B} = (Z_{A,A} + Z_{B,B} - 2Z_{A,B})^{1/2}. \quad (6)$$

We also examine the variation of two further parameters, α and β, also defined first by Cioslowski [16]. The isosynchronicity parameter, α, is given by

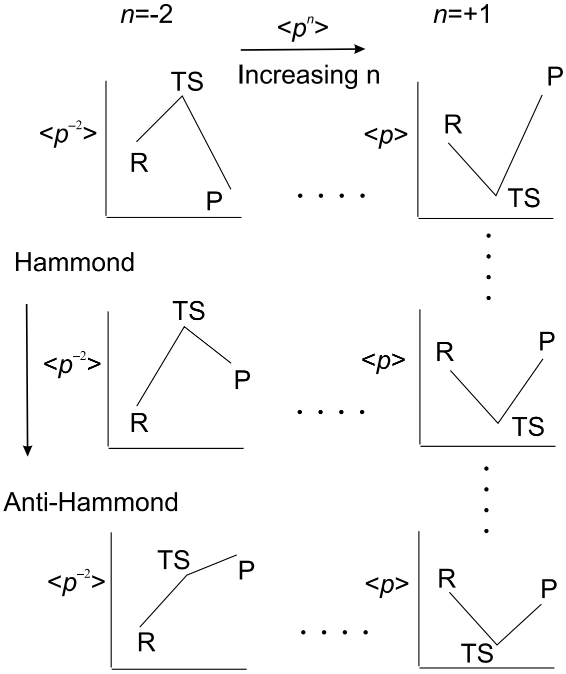

Fig. 2. Schematic variation of $\langle p^n\rangle$ along the reaction coordinate for Hammond and anti-Hammond reactions. R, TS and P denote reactants, transition state and products, respectively.

$$\alpha = (d_{R,TS} + d_{P,TS})/d_{R,P}, \quad (7)$$

and is never smaller than 1. It takes a value close to one when the distance from either R or P to the TS is small or when the transition state loses similarity to the reactants in the same way as it gains similarity to the products. The structural proximity of the transition state to the reactants is given by β, defined by

$$\beta = (d_{R,TS} - d_{P,TS})/d_{R,P}, \quad (8)$$

and which takes values between −1 and 1. If reactants and transition state are closer than the products to the TS, then the TS is early and $\beta < 0$. Positive values of β correspond to a late TS.

We have found it useful to define two new parameters, δ and ϕ, calculated from $d_{R,TS}$, $d_{P,TS}$ and $d_{R,P}$. As shown in Fig. 3, we can depict any reaction by a triangle with vertices representing reactant, product and the transition state and sides equal in length to the values of d. Triangles skewed to the right or left indicate late or early transition states, respectively. A relatively long base suggests

Table 3
r-Space Coulomb similarity indices and distances, and values of the parameters α, β, δ and ϕ, as defined in the text

Reaction	$I_{R,P}$	$I_{R,TS}$	$I_{P,TS}$	$d_{R,P}$	$d_{R,TS}$	$d_{P,TS}$	α	β	δ	ϕ
(a) HF										
F_2S_2/FSSF	0.925	0.939	0.916	14.36	12.94	15.17	1.96	−0.155	−0.086	0.338
HNC/HCN	0.997	0.998	0.997	0.849	0.815	0.894	2.01	−0.092	−0.051	0.330
H_2SO/HSOH	0.982	0.980	0.999	4.40	4.71	1.05	1.31	0.832	0.490	0.370
H_2SCH_2/$HSCH_3$	0.990	0.962	0.967	3.17	6.21	5.74	3.78	0.146	0.091	0.169
(b) DFT										
F_2S_2/FSSF	0.932	0.944	0.933	13.61	12.31	13.45	1.89	−0.084	−0.046	0.353
HNC/HCN	0.998	0.998	0.997	0.844	0.784	0.876	1.97	−0.109	−0.060	0.338
H_2SO/HSOH	0.980	0.982	0.999	4.65	4.46	0.72	1.11	0.804	0.343	0.560
H_2SCH_2/$HSCH_3$	0.991	0.972	0.979	3.05	5.29	4.56	3.24	0.239	0.146	0.195

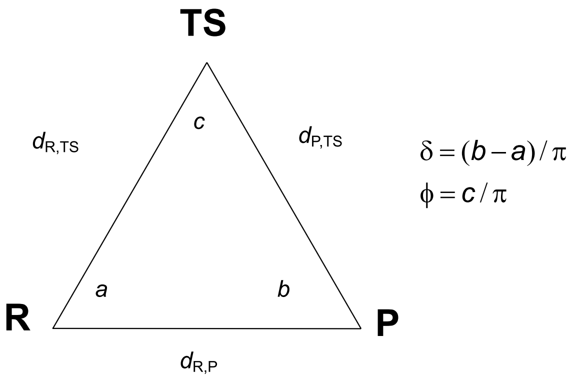

Fig. 3. Definition of the parameters δ and ϕ.

large changes in structure accompanying the reaction, and a tall triangle suggests significant structural differences between the transition state and the reactants and products. We define δ and ϕ in terms of the angles (in radians) subtended at the reactants, products and transition state, as shown in Fig. 3. The parameter δ, which takes values between −1 and 1, is a measure of whether the transition state is early or late. A reaction with an early transition state will have a negative value of δ. For given δ, the value of ϕ $(0 \leqslant \phi \leqslant 1)$ indicates how far the transition state lies from reactants/products.

Table 3 collects together α, β, δ and ϕ for the four reactions. The δ parameters follow the order:

$$\underset{\text{Early TS}}{\mathrm{HNC/HCN}} \approx \mathrm{F_2S_2/FSSF} < \mathrm{H_2SCH_2/HSCH_3} < \underset{\text{Late TS}}{\mathrm{H_2SO/HSOH}}$$

This is the same trend as obtained with the momentum–space expectation values. The values of ϕ for the isoelectronic H_2SCH_2/$HSCH_3$ and H_2SO/HSOH reactions reflect the very different structures of the transition states [14], and the relative distance of the transition state from reactants and products. In the H_2SCH_2/$HSCH_3$ rearrangement, the S–C bond length increases considerably (>0.5 Å at both HF and DFT levels) from the reactant to the transition state before contracting markedly to a final value much closer to the original. H_2SCH_2/$HSCH_3$ is the only one of the four reactions in which the similarity of reactant and product is larger than either the similarity between reactant and TS or product and TS, and this is ultimately the origin of the small value of ϕ. This is reflected also in the large values of $\Delta\langle p^{-1}\rangle$ involving this transition state (see Table 2). An analogous variation in the length of the stiffer S–O bond is not observed in the H_2SO/HSOH reaction.

Unlike in the series of proton transfer reactions studied by Cioslowski [16], we find here no correlation between β and γ, which decreases from reaction (A) to reaction (D) (Table 1). In addition there is no correlation between γ and any of α, β or ϕ. The reactions we have studied are, overall, too dissimilar.

4. Conclusions

The changes in moments of momentum and in *r*-space similarity indices between reactant, product and transition state can be used to distinguish between Hammond and anti-Hammond behaviour. Two new parameters, δ and ϕ, have also been introduced to quantify the position and character of the transition state relative to the reactants and products. Together, these quantities provide a concise quantitative description of transition states and a convenient means for examining the relationships between reactants, products and transition state. We now aim to use similar ideas to examine transition states in more complex systems involving enzymes.

Acknowledgements

This work was carried out during a stay of DLC and NLA in Girona made possible by a CESCA grant from the Computing Centre, University of Barcelona, and they would like to thank RC-D for his hospitality throughout this and other visits.

References

[1] For example, I.R. Epstein, A.C. Tanner, in: B.G. Williams (Ed.), Compton Scattering, McGraw-Hill, New York, 1977 (Chapter 7).

[2] D.C. Rawlings, E.R. Davidson, J. Phys. Chem. 89 (1985) 969.

[3] P.T. Measures, N.L. Allan, D.L. Cooper, Int. J. Quant. Chem. 60 (1996) 579.

[4] N.L. Allan, D.L. Cooper, J. Chem. Soc., Faraday Trans. 2 (83) (1987) 449.

[5] D.L. Cooper, N.L. Allan, P.J. Grout, J. Chem. Soc., Faraday Trans. 2 (85) (1989) 1519.

[6] E. Besalú, R. Carbó, J. Mestres, M. Solà, Top. Curr. Chem. 173 (1995) 31.

[7] R. Carbó-Dorca, E. Besalú, J. Mol. Struct. (Theochem) 451 (1998) 11.

[8] Ll. Amat, R. Carbó-Dorca, R. Ponec, J. Med. Chem. 42 (1999) 5169.

[9] R. Carbó-Dorca, D. Robert, Ll. Amat, X. Gironés, E. Besalú, in: Molecular Quantum Similarity in QSAR and Drug Design, Lecture Notes in Chemistry, vol. 73, Springer, New York, 2000.

[10] For example, D.L. Cooper, K.A. Mort, N.L. Allan, D. Kinchington, C. McGuigan, J. Am. Chem. Soc. 115 (1993) 12615.

[11] P.T. Measures, K.A. Mort, N.L. Allan, D.L. Cooper, J. Comput-Aided Mol. Des. 9 (1995) 331.

[12] N.L. Allan, D.L. Cooper, J. Math. Chem. 23 (1998) 51.

[13] G.S. Hammond, J. Am. Chem. Soc. 77 (1955) 334.

[14] M. Solà, J. Mestres, R. Carbó, M. Duran, J. Am. Chem. Soc. 116 (1994) 5909.

[15] M.J. Frisch et al., GAUSSIAN 98, Revision A.6, Gaussian Inc., Pittsburgh, PA, 1998.

[16] J. Cioslowki, J. Am. Chem. Soc. 113 (1991) 6756.

[17] N.L. Allan, D.L. Cooper, Top. Curr. Chem. 173 (1995) 85.

[18] V.N. Staroverov, E.R. Davidson, Mol. Phys. 99 (2001) 175.

[19] P. Duffy, D.P. Chong, M.E. Casida, D.R. Salahub, Phys. Rev. A 50 (1994) 4707.

[20] For example, R. Carbó, M. Arnau, L. Leyda, Int. J. Quant. Chem. 17 (1980) 1185.

[21] R. Carbó, B. Calabuig, Int. J. Quant. Chem. 42 (1992) 1681.

[22] P. Constans, L.L. Amat, R.R. Carbó-Dorca, J. Comput. Chem. 18 (1997) 826.